

# AERODYNAMICS OF THE F-15 AT HIGH ANGLE OF ATTACK

Shuchi Yang<sup>1</sup>, P.C. Chen<sup>1</sup>, X.Q. Wang<sup>2</sup>, Marc P. Mignolet<sup>2</sup>, and Dale M. Pitt<sup>3</sup>

<sup>1</sup>ZONA Technology, 9489 E. Ironwood Square Drive, Scottsdale, AZ 85258

<sup>2</sup>SEMTE, Faculties of Mechanical and Aerospace Engineering, Arizona State University,  
Tempe, AZ 85287-6106

<sup>3</sup>Boeing Research & Technology (BR&T), Smart Structures and Systems, St. Louis, MO.

## Abstract

In this paper, the unstructured-grid flow solver, FUN3D, is used to compute the aerodynamic performance of F-15. A half model of F-15 with 14 million grid points is used for both steady and unsteady computations. The Detached Eddy Simulation (DES) method based on the Spalart-Allmaras (SA) turbulence model is used in the unsteady computation of the F-15 with high angle of attack. Computational results for the transonic steady cases of the F-15 vertical tail and the benchmark case of a cylinder in a cross flow are presented, showing excellent agreement with other numerical results and experimental measurements in the literature. Furthermore, unsteady pressure fluctuations on the F-15 vertical tail at a high angle of attack ( $22^\circ$ ) are computed. The effect of the far field turbulence on the power spectrum of the pressure is studied, and the optimal turbulence level is determined to capture the dominant regime of the power spectrum of the pressure measured in wind tunnel tests. The FUN3D computation is thus expected to provide reliable pressure data for the prediction of the buffeting response of the F-15 vertical tail.

## 1. Background

For high performance aircraft, such as F-15 and F/A-18, vortex emanating from wing leading edge extension (LEX) often burst at high angle of attack which usually immerses on the vertical tail in the wake. Although these vortices often increase lift, the resulting unsteady pressure associate with the separated flow, which is named buffet, on the vertical tail introduces fatigue crack. This phenomenon, along with the aeroelastic coupling of the tail structural assembly, results in vibrations that can shorten the fatigue life of the empennage assembly and limit the flight envelope due to the large amplitude of the fin vibrations. Among twin-tail fighter aircrafts, tail buffet was first noticed through its destructive effects of induced fatigue cracks in the F-15 aircraft. The fatigue cracked were notice shortly after the F-15 was placed service and many high angles of attack maneuvers were executed.

The buffeting of the F-15 at high angle of attack induces vibrations of its vertical tails and thus is a concern in particular from the standpoint of fatigue. The computational prediction of the buffeting loads on the aircraft is a particularly challenging task owing to the random unsteady character of the resulting pressure field, e.g. see [1, 3]. The complexity of the flow field has motivated a series of wind and water tunnel experiments the measurements of which are important validation data. Further experimental studies have been done to alleviate the buffet by different method [6-9]. Due to the development of computational technique and computational algorithm, more and more investigation has been done by computational fluid dynamics tools to investigate the buffet phenomena of the twin-tail fighter, e.g., F-15 and F/A-18. [1-5, 10].

At the first stage, the researcher focused on the computational on simpler geometries, such as slender fore-bodies and delta wings, to improve their simulation capabilities. However, the advent of hybrid turbulence models may finally allow for the accurate prediction of full aircraft flow fields at high incidence.

At second stage, with the advances of grid generation and fast algorithms for solutions of systems of equations, CFD has remained limited as a reliable tool for prediction of inherently unsteady flows at flight Reynolds numbers. The Reynolds-averaged Navier-Stokes (RANS) equations are solved for unsteady flow with turbulence models to necessarily model the entire spectrum of turbulent motions. Since most time adequate in steady flows with no regions of reversed flow, or possibly exhibiting hallow separation, it appears inevitable that RANS turbulence models are unable to accurately predict flows characterized by massive separation.

At third stage, in order to overcome the deficiencies of RANS models for predicting massively separated flows, Spalart et al.[11] proposed Detached Eddy Simulation (DES) with the objective of developing a numerically feasible and accurate approach combining the most favorable elements of RANS models and Large Eddy Simulation (LES). The main advantage of DES is that it can be applied at high Reynolds numbers, as can Reynolds-averaged techniques, but DES also resolves geometry-dependent, unsteady three-dimensional turbulent motions as in LES.

The focus of the present investigation is on the validation of the unstructured CFD solver FUN3D for the prediction of the high angle of attack flow on the F-15 including both steady and unsteady, i.e. buffeting. The paper is arranged as following.

- (i) Computational method and computational grid are discussed.
- (ii) The validation of the steady aerodynamics on the F-15 at high angle of attack predicted by FUN3D with wind tunnel measurements
- (iii) The validation of the detached eddy simulation capability of FUN3D on a benchmark case, i.e., the fluctuating pressure field behind a cylinder, in comparison with wind tunnel data and other CFD results
- (iv) the validation of the unsteady pressure fluctuations on the F-15 vertical tail during buffeting with wind tunnel measurements.

## **2. Computational Methodology**

### ***A. Flow solver***

In this paper, the FUN3D code from NASA LARC is used to perform the steady and time-accurate simulation. In FUN3D, the cell-vertex finite volume method is used to discretize the Reynolds-Averaged Navier-Stokes (RANS) equation with unstructured grid. For steady flow, the local time step is used to accelerate the convergence, and the dual time method is used for unsteady computation with second-order back-difference, point-implicit algorithm. In order to deal with complex configuration, several different types of grid elements (tetrahedrons, pyramids, prisms, and hexahedrons) can be accommodated into the computational mesh. Different inviscid upwind flux schemes with various flux limiters are available. In order to further reduce the computational time, the computational domain is divided into multiple parts and MPI are used for parallel computation with distributed memory systems.

### ***B. Turbulence Models***

There are plenty of choices in FUN3D for turbulence models. For steady calculations, we mainly use one-equation Spalart-Allmaras (SA) [11] mode in conjunction with the solid-body rotation modification of Dacles-Mariani et al [2]. For unsteady simulations, following Vatsa et al., a modified Delayed Detached Eddy Simulation methodology was utilized [12]. In the original DDES, a hybrid approach that uses the RANS equations with the Spalart-Allmaras model near the wall and a switching function to transition to the LES region in the rest of the computational domain is used. In the DDES model, a blending function is applied to the destruction terms in the turbulence equation. In MDDES, the blending function is also applied to the production terms, but only outside of the near-wall region. As with any hybrid RANS/LES approach, the results obtained with this methodology are sensitive to characteristics of the flow solver, turbulence model, and overall grid topology used.

### C. Computational Grids

Figure 1 presents the unstructured mesh for a half-span computational model of the F-15 provided by Boeing. It consists of 14,045,325 grid points, 12,536,743 hexahedral volume elements, 110,658 pentahedral volume elements with five nodes (pyramid), and 23,371,777 pentahedral volume elements with six nodes (prismatic). The half-span model is sufficient for the present effort as only buffeting due to high angle of attack will be considered here which produces a symmetric flow about the aircraft mid-plane.

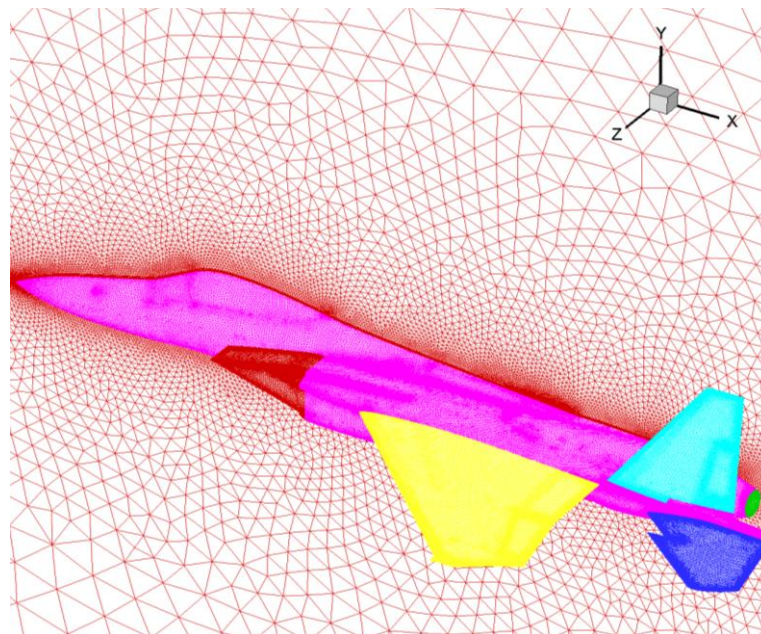


Figure 1. F-15 unstructured mesh.

In addition to the mesh, appropriate boundary conditions on each region of the model have been identified and imposed in the FUN3D boundary conditions including:

- (i) the mass-flow-in condition on the inlet face
- (ii) the symmetry condition on the mid-plane to enforce the symmetric flow solution
- (iii) the mass-flow-out boundary condition on the surface mesh of the exhaust nozzle
- (iv) the far field boundary condition, using the Riemann invariants method
- (v) strong enforcement of the no-slip boundary condition on the viscous walls.

### 3. F-15 Steady Characteristics at High Angle of Attack

Wind tunnel measurements on the F-15 were provided by Boeing. These measurements were performed in the MDC Polysonic Wind Tunnel, a blow-down atmospheric tunnel with a 4 x 4 foot test section, in 1971. Figure 2 presents the comparison of lift ( $C_L$ ) vs. angle of attack ( $\alpha$ ) at Mach number ( $M_\infty$ ) = 0.95 between the FUN3D solution and the wind tunnel data.

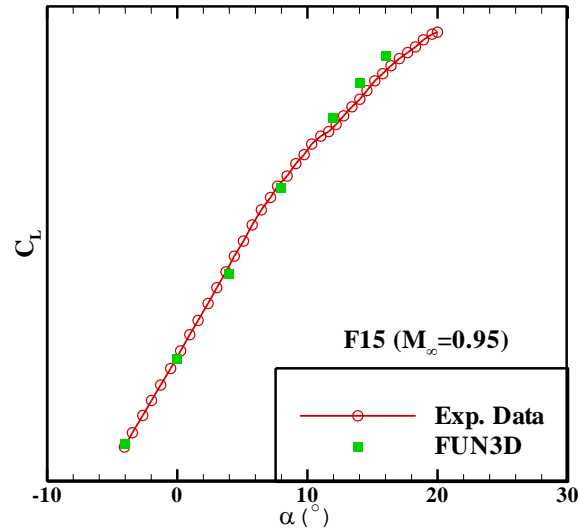


Figure 2. Lift ( $C_L$ ) vs. angle of attack ( $\alpha$ ) at Mach number ( $M_\infty$ )=0.95 of F-15.

It can be seen from Fig. 2 that  $C_L$  is linearly varying with  $\alpha$  only up to  $\alpha=10$  degrees indicating that large flow separation occurs at  $\alpha > 10$  degrees. The FUN3D solution agrees very closely with the wind tunnel measurements for the entire range of angle of attack. These results present a first successful validation of FUN3D for F-15 steady aerodynamics at high angle of attack where large flow separation occurs.

Next is the detailed comparison of the pressure distribution on the F-15 at various flow conditions between FUN3D and the wind tunnel measurements. The analyzed flow conditions are given in Table 1 and the corresponding comparisons are shown in Figs. 3 to 6. In the left and right upper corners of these figures are the FUN3D computed pressure contours on the upper and lower surfaces of the F-15, respectively, while the figures beneath them are the pressure distributions comparisons at the six span wise stations on the wing between FUN3D solution and the wind tunnel measurements.

Table 1 Flow Conditions for pressure comparison on F-15

Mach Number	Angle-of-Attack (deg.)	Figure Number
0.606	4.36	3
0.609	15.12	4
0.899	4.84	5
0.900	11.92	6

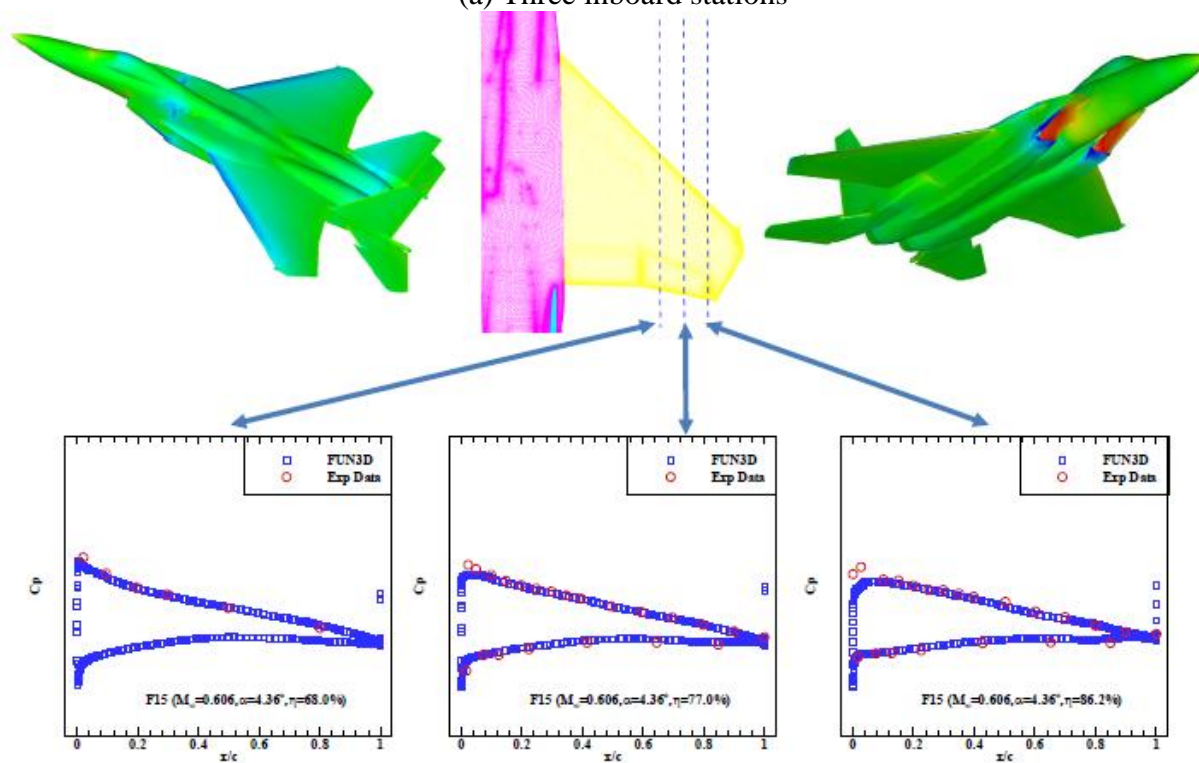
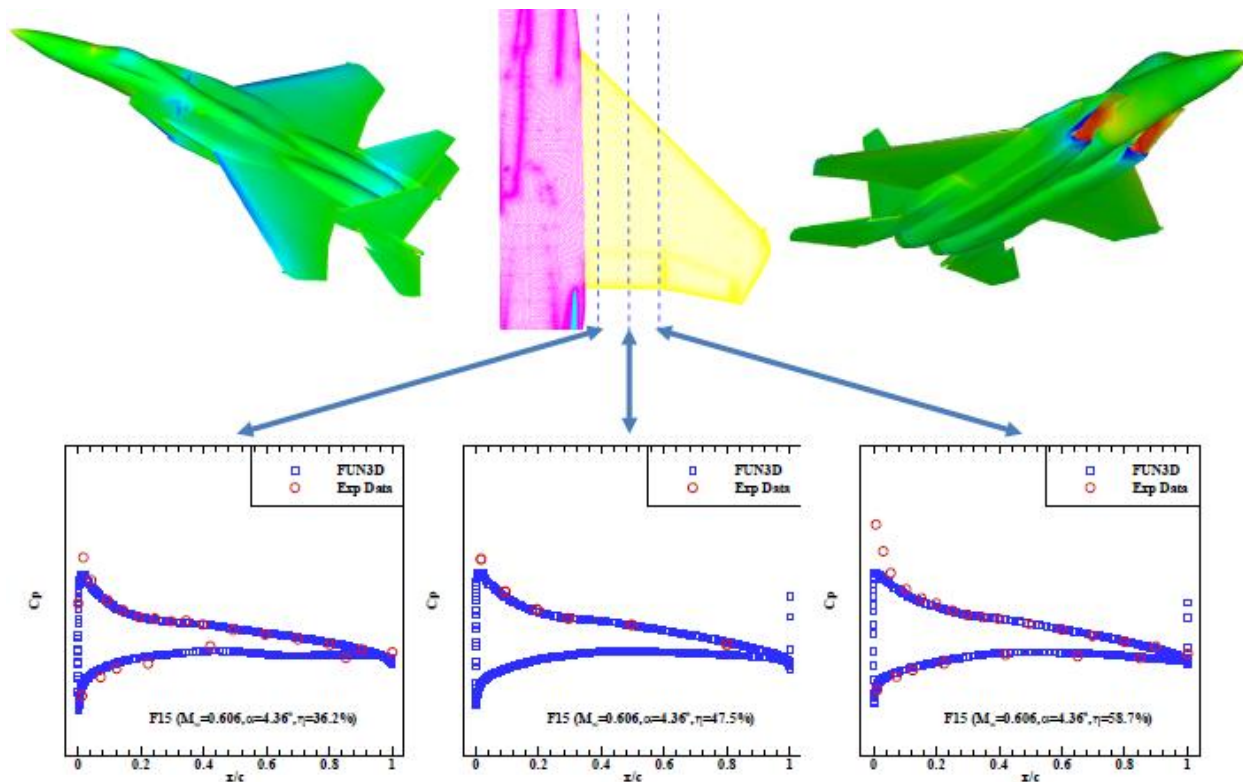
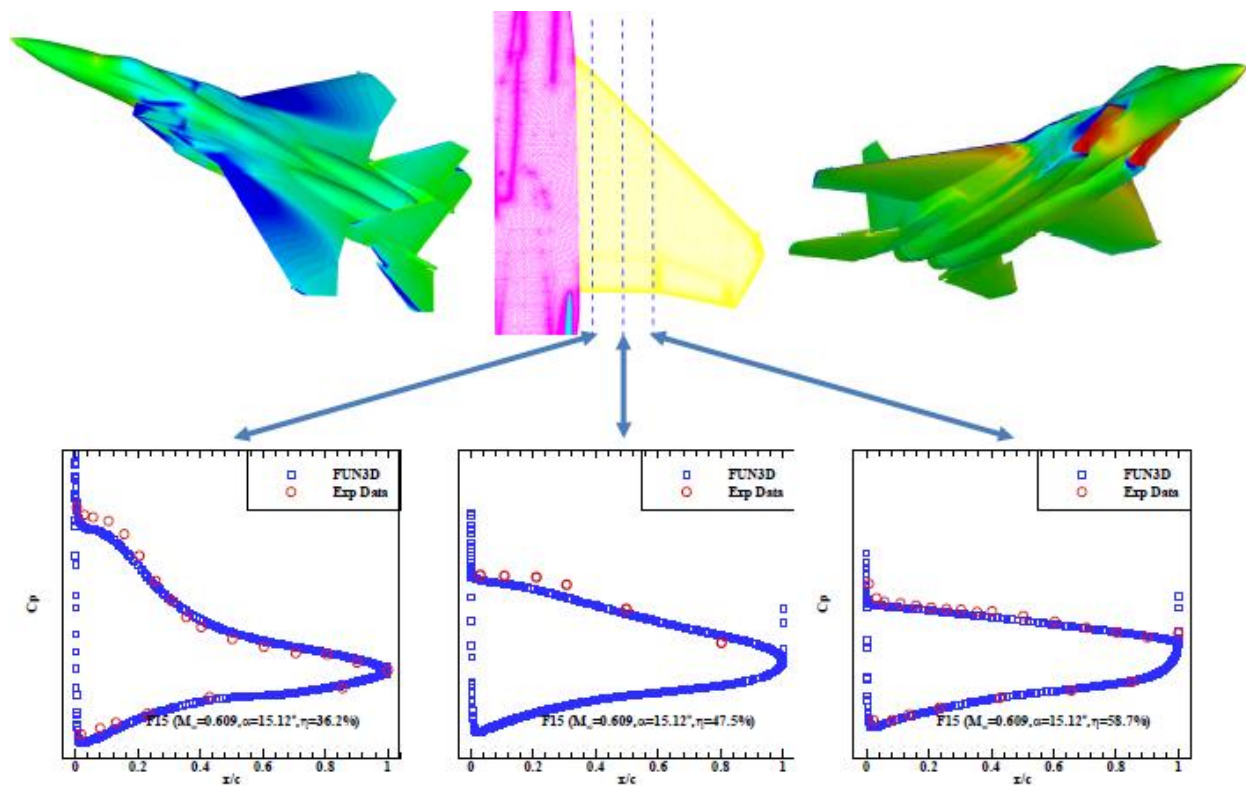
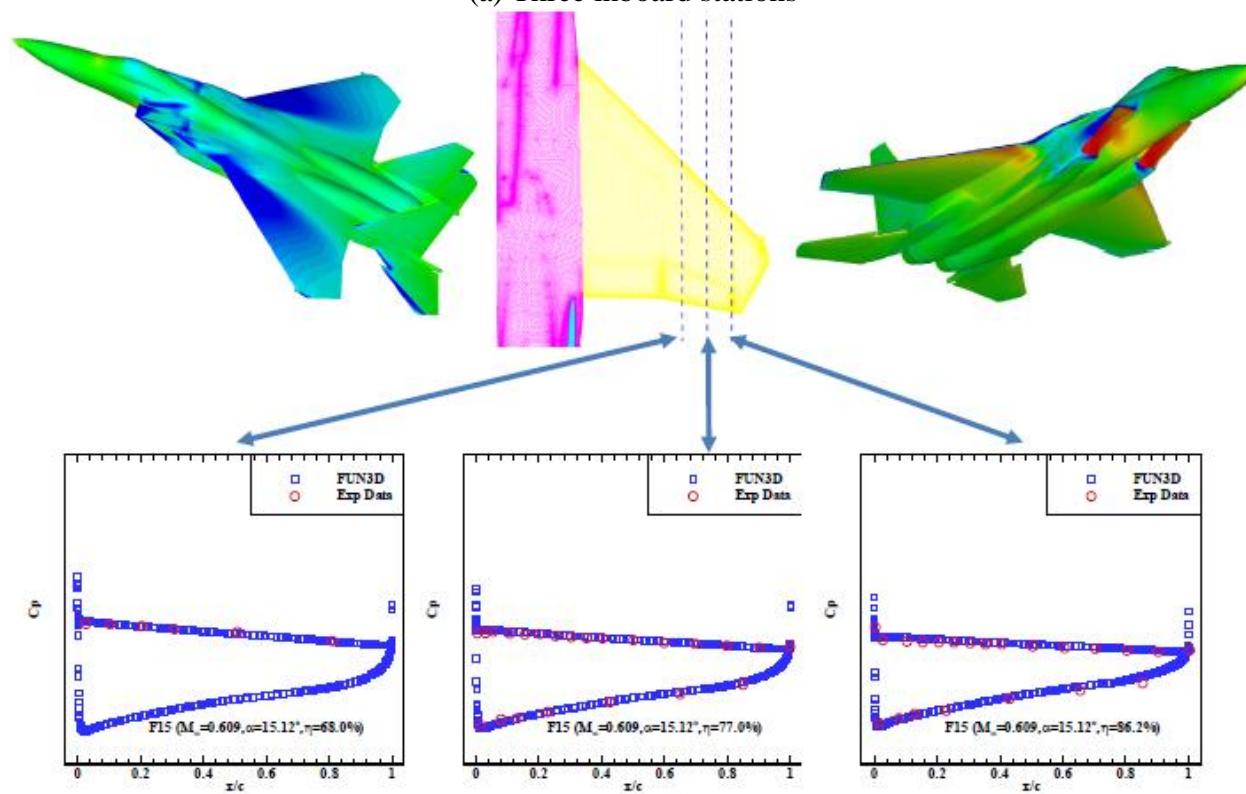


Figure 3. Pressure distributions on F-15 at  $M_\infty = 0.606$  and  $\alpha = 4.36^\circ$

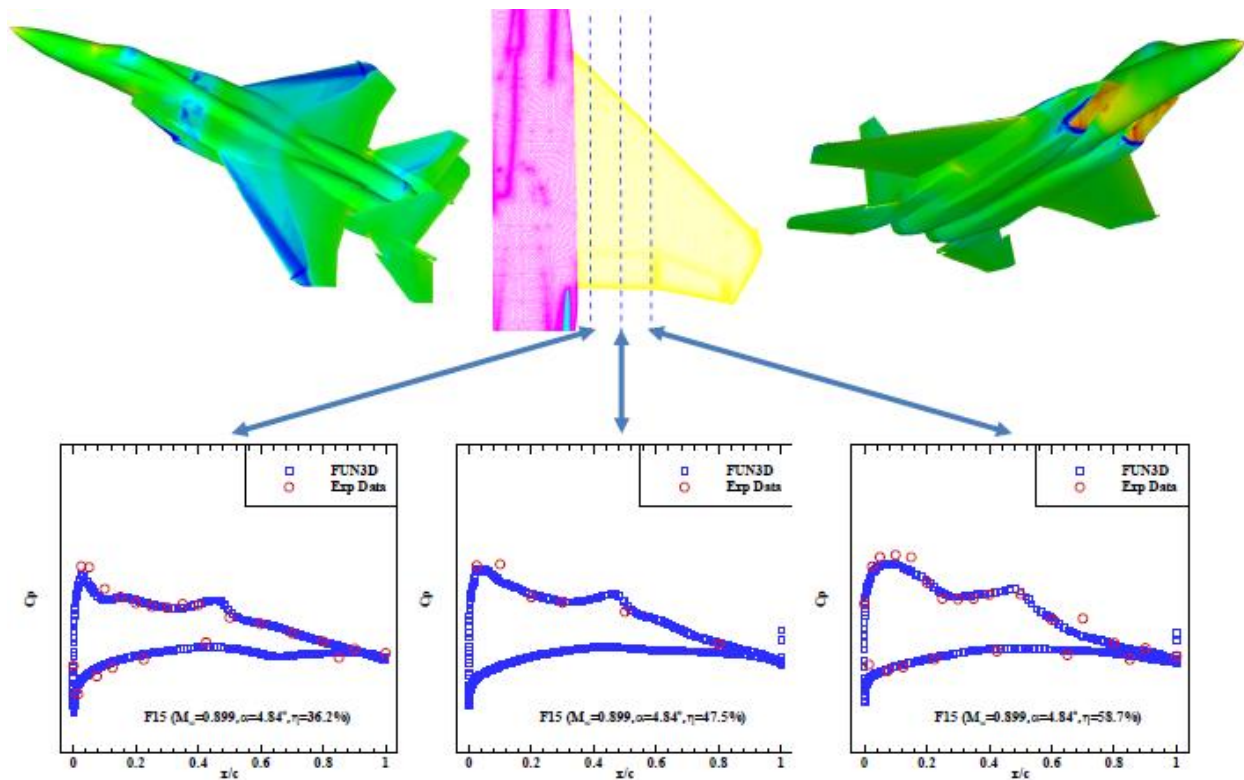


(a) Three inboard stations

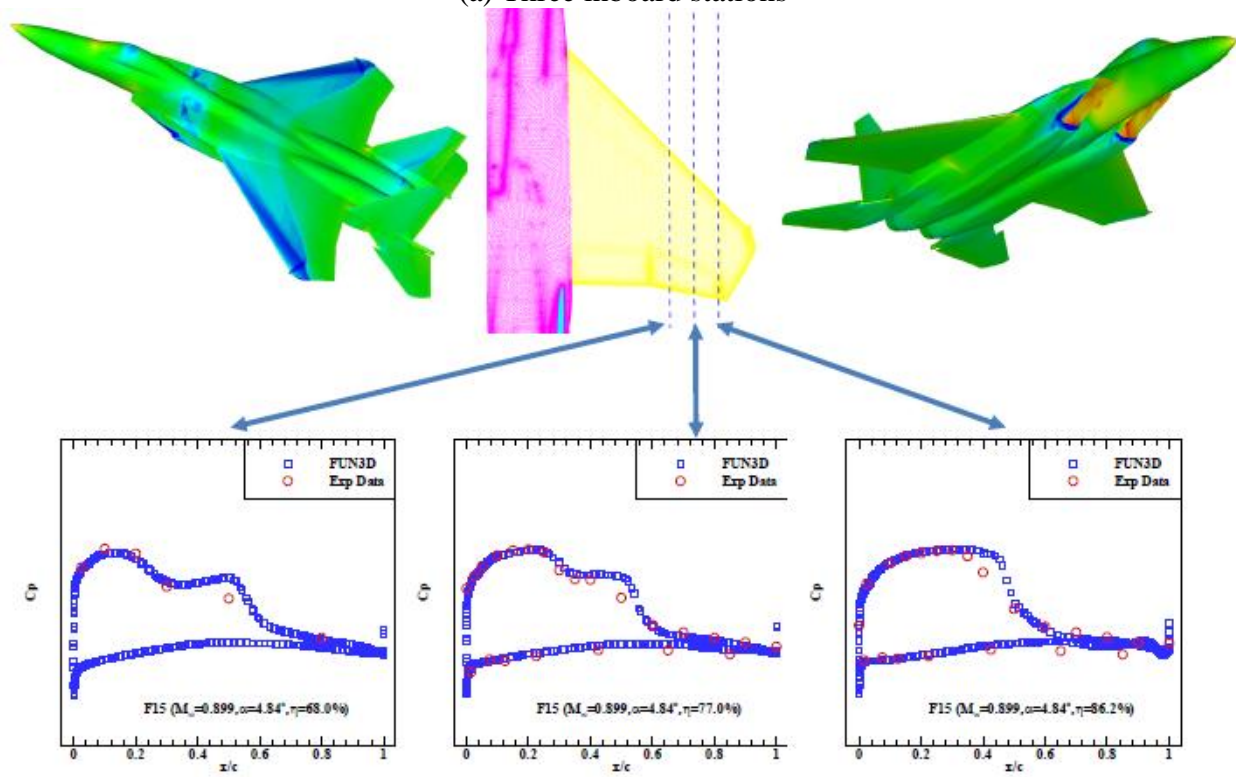


(b) Three outboard stations

Figure 4. Pressure distributions on F-15 at  $M_\infty = 0.609$  and  $\alpha = 15.12^\circ$

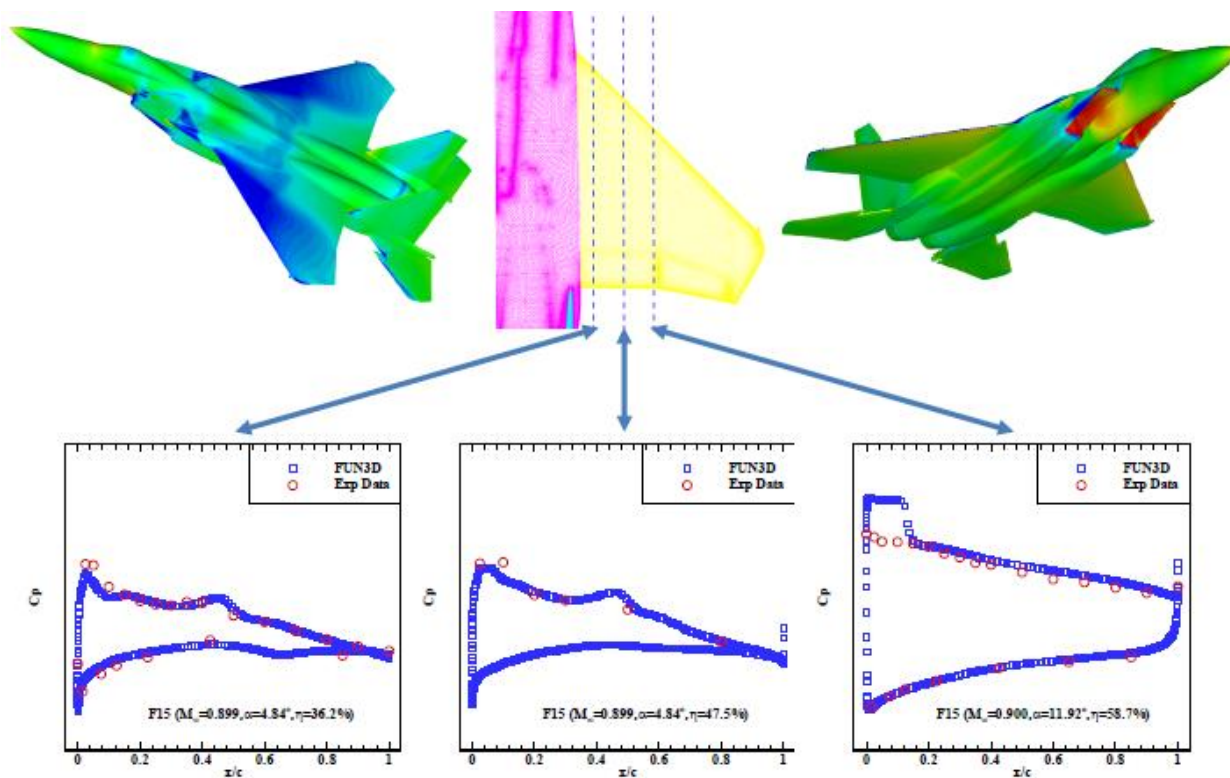


(a) Three inboard stations

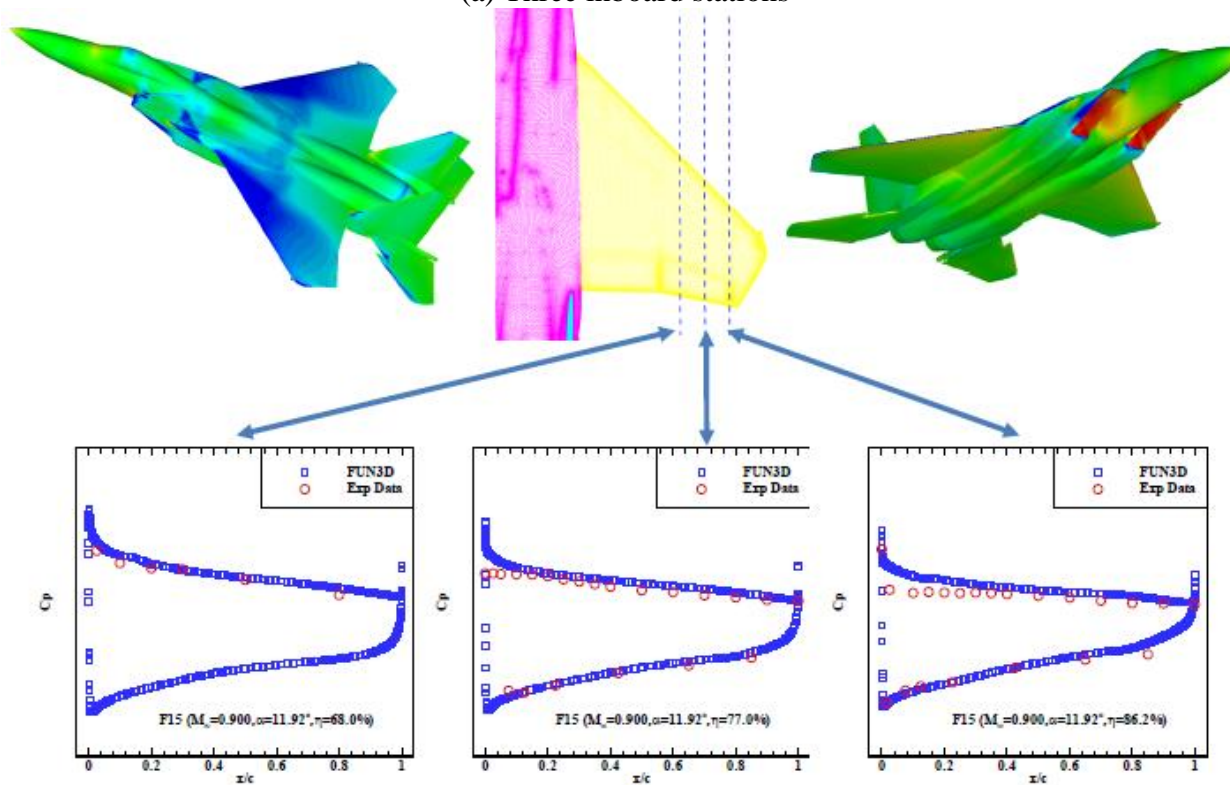


(b) Three outboard stations

Figure 5. Pressure distributions on F-15 at  $M_\infty = 0.899$  and  $\alpha=4.84^\circ$



(a) Three inboard stations



(b) Three outboard stations

Figure 6. Pressure distributions on F-15 at  $M_\infty = 0.900$  and  $\alpha = 11.92^\circ$

Figure 3 shows the pressure distribution comparison at  $M_\infty = 0.606$  and  $\alpha=4.36^\circ$ . This is a low Mach number and low angle of attack condition, therefore it is expected that the FUN3D solution should agree closely with the wind tunnel measurements, as is indeed shown on Fig. 3. At the approximately the same Mach number but angle of attack increased to  $15.12^\circ$ , see Fig. 4, it is expected that large flow separation occurs, especially at the outboard region on the upper surface of the wing. The wind tunnel measurements verify this occurrence of large separation as evidenced by the flat  $C_p$  distribution on the upper surface of the wing shown on Fig. 4(b). This large flow separation is captured very well by FUN3D. Figure 5 shows the pressure distribution comparison at  $M_\infty = 0.899$  and  $\alpha=4.84^\circ$ . This is a transonic flow condition at low angle of attack and thus transonic shocks should occur. These transonic shock strengths and locations are very well captured by FUN3D as evidenced by the good pressure distribution agreement with the wind tunnel measurements. At approximately the same Mach number but angle of attack increased to  $11.92^\circ$ , see Fig. 6, it is expected large flow separation occurs at the outboard sections of the wing while transonic shocks are still present in the inboard section of the wing. This mixed flow distribution is a challenging case to be captured by the computational method but FUN3D performs very well and a good agreement with wind tunnel measurements is shown in Fig. 6.

#### 4. Validation of FUN3D of a Cylinder in a Crossflow

The above successful comparison of FUN3D with steady aerodynamic wind tunnel measurements of the F-15 was obtained using the pseudo time marching scheme in FUN3D. However, capturing the buffeting flow, which is a naturally occurring fluctuation, requires an accurate time marching scheme with detached eddy simulation capability. For the unsteady computation, the first-order time-accurate algorithm is used to setup a quasi-stable solution, after that the 2nd-order time-accurate algorithm will be applied for the FUN3D with DES option. This method can reduce the computational time than conduct 2nd-order computation from the beginning.

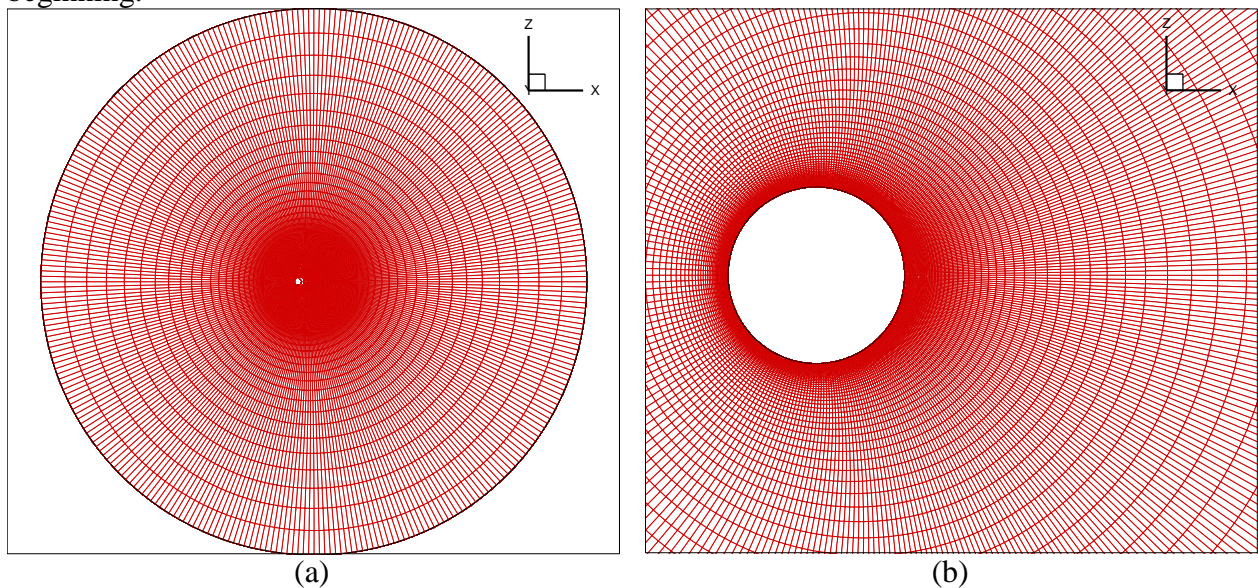


Figure 7. FUN3D Computational grid for the cylinder in crossflow benchmark case.

The standard benchmark case for validation of detached eddy simulation scheme is the cylinder in a crossflow condition at  $M_\infty=0.3$  and a Reynolds number ( $Re$ ) of  $1.4E5$ . The length to

diameter ratio of the cylinder considered here is 4. Figure 7 presents the computational mesh for this problem, which includes  $317 \times 113 \times 41$  grid points and about 1,500,000 hexahedron cells. Further, periodic boundary conditions are used on both sides of the cylinder.

Shown in Fig. 8 are the time-averaged pressure coefficient and skin friction coefficient distributions around the circumference of the mid-plane of the cylinder as predicted by FUN3D and by the computational study of Krishnan et al. [13] along with some experimental measurements obtained by Roshko [14] (for  $Re = 8.5 \times 10^6$ ) and Van Nunen [15] (for  $Re = 7.6 \times 10^6$ ). On the windward side, the pressure coefficient distributions among the computational results and experimental data all agree well as expected given the attached flow condition. On the leeward side which is immersed in the separated flow, an excellent agreement is still obtained between FUN3D and the predictions of Krishnan et al. [13]. However, large differences between these two sets of experimental data can be seen in spite of the small difference (about 10%) in Reynolds number. This data clearly indicates the high sensitivity of the separated flow characteristics to small variations in flow conditions such as wind tunnel wall effects, turbulence intensity of the oncoming flow, etc. These results further highlight the difficulty in performing a one-to-one comparison between computational results and experimental measurements that is inherent in detached flows.

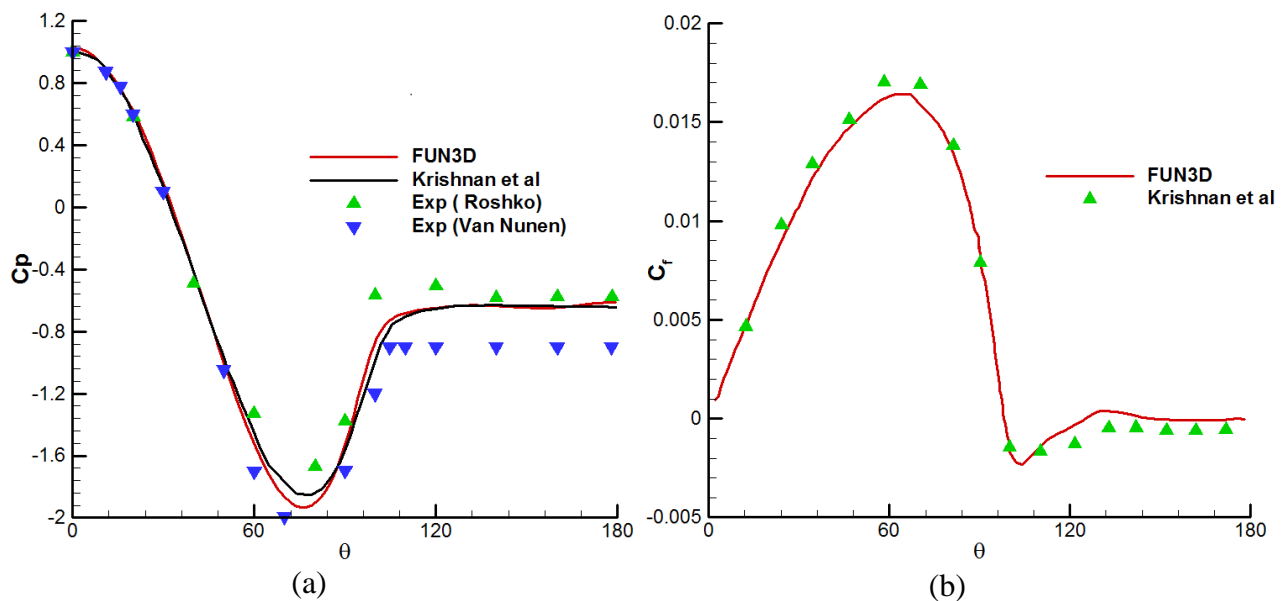


Figure 8 Time averaged values of (a) the pressure coefficient ( $C_p$ ) and (b) the skin friction ( $C_f$ ) coefficient around the circumference of the mid-plane of the cylinder

Note that the separated flow is oscillatory as shown by the FUN3D lift and drag friction coefficients time history shown in Fig. 9. The results of Fig. 8 were obtained by a time averaging approach of those time histories as is current practice but this process can also be the source of discrepancies between computational results and experimental data.

Figure 10 shows the vorticity and non-periodic vortex shedding behind the cylinder at selected time steps computed by FUN3D. The accuracy in determining these vorticity and vortex shedding in the separated flow is of primary importance for the prediction of buffet loads on a downstream structural component. In the present context, the buffet loads on the F-15 vertical

tail result directly from the vorticity/vortex shedding from the upstream wings and the strakes which thus must be predicted accurately.

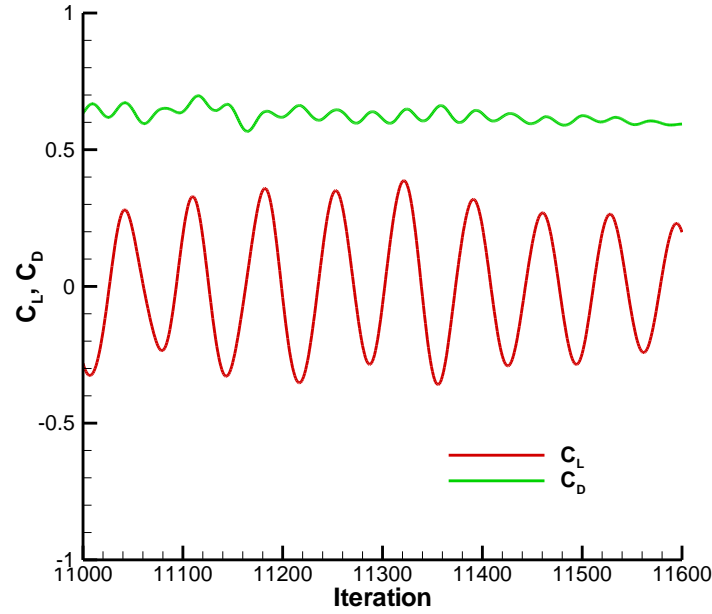


Figure 9 Time histories of lift ( $C_L$ ) and drag ( $C_D$ ) coefficients of the cylinder obtained by FUN3D.

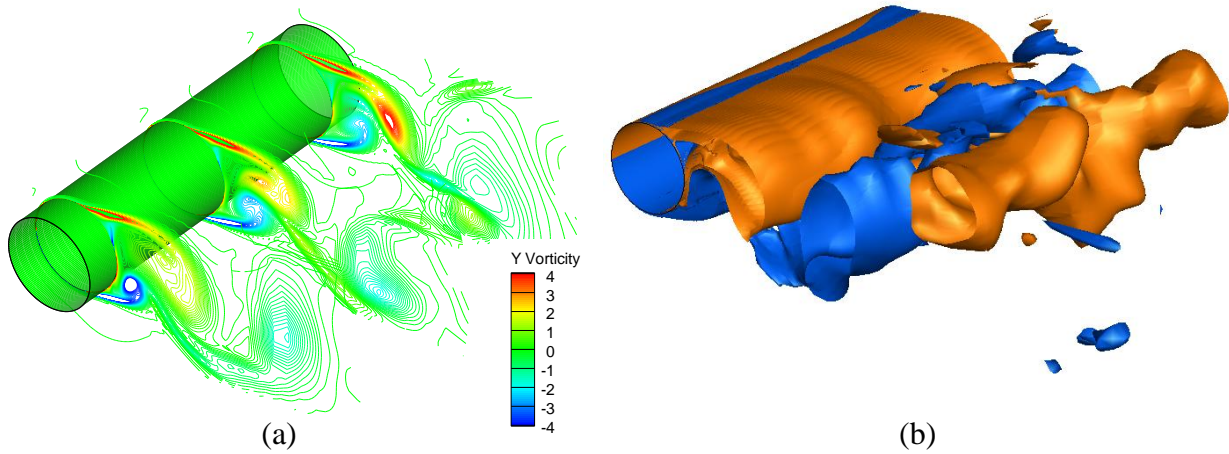


Figure 10. (a) Vorticity and (b) vortex shedding behind the cylinder computed by FUN3D.

Table 2 Comparison of flow characteristics on cylinder

	$C_D$	St	$-C_{pb}$	$\theta_{sep}$
FUN3D	0.60	0.278	0.64	$99^\circ$
Krishnan et al. [13]	0.60	0.28	0.69	$99^\circ$
Travin et al. [16]	0.57	0.30	0.65	$99^\circ$
Hansen et al. [17]	0.59	0.29	0.72	-

Roshko [14]	0.62~0.74	0.27	-	-
-------------	-----------	------	---	---

As a final assessment of FUN3D in this cylinder in a crossflow benchmark problem, shown in Table 2 are the drag coefficient ( $C_D$ ), Strouhal number ( $St$ ), pressure in separation region ( $C_{pb}$ ), and separation angle on the cylinder ( $\theta_{sep}$ ) computed by FUN3D, other numerical analyses ([13,16-17]), and measured in wind tunnel test [14]. This excellent agreement of FUN3D results with other available data demonstrates that the detached eddy simulation capability in FUN3D can accurately predict the fluctuating flow due to large flow separation and is ready for the buffet load study on the F-15 vertical tail.

### 5. Validation of the Unsteady Pressure Fluctuations on the F-15 Vertical Tail During Buffeting with Wind Tunnel Measurements

The wind tunnel test [18] for measuring the buffet responses of the F-15 vertical was conducted on a 13% scale model of the F-15 in the MACAIR Low Speed Wind Tunnel (LSWT). The wind tunnel experiment was conducted at a Mach number  $M_\infty = 0.09$ , a dynamic pressure of 12 psf, and a Reynolds number  $Re = 6.8 \times 10^5$  per ft. The right vertical tail was instrumented with 39 pressure transducers on both the inboard and the outboard sides (see Fig. 11), and the power spectral densities of the pressure at an angle of attack of  $22^\circ$  were measured.

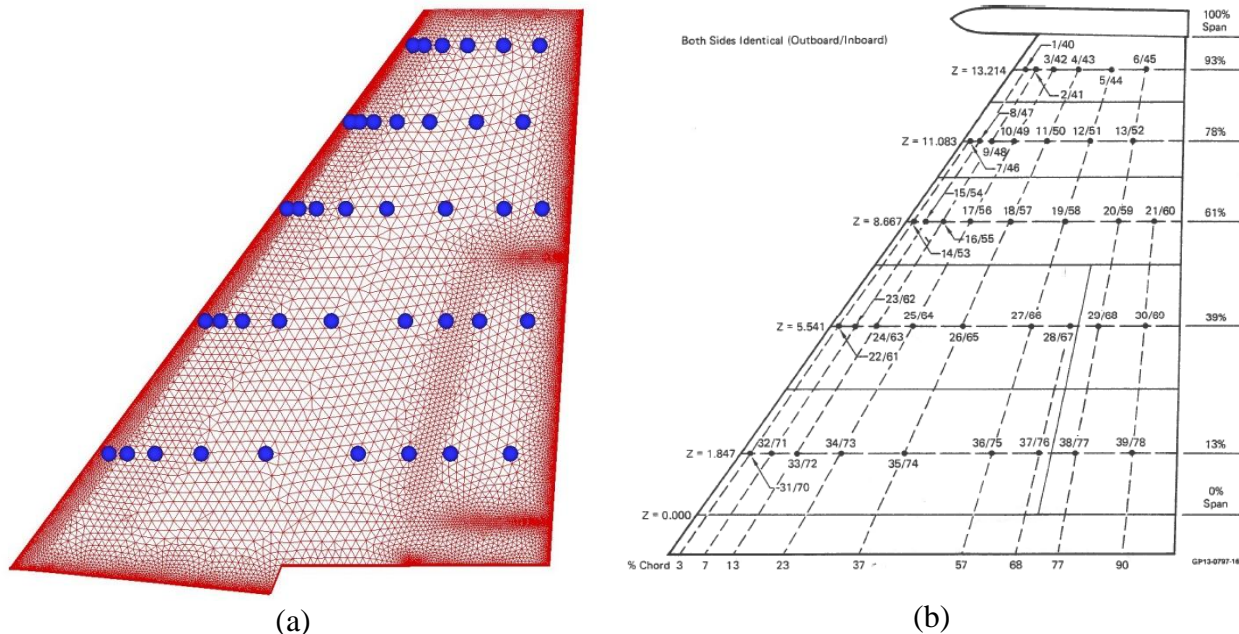


Figure 11. Location of the sensors on the right vertical tail. (a) with respect to the FUN3D mesh. (b) Physical locations (from [18]).

The FUN3D computations were carried out with a physical time step of  $2.78 \times 10^{-4}$  seconds, see Fig. 12 for a sample time history. A key input in the FUN3D computations is the level of upstream turbulence which was not provided in [18] for the experiments. It was found that varying this level led to notably different power spectra of the pressures, as seen from Figs. 13 and 14. The turbulence level of 3.0 was finally adopted as it led to a good capture of the dominant frequency regime of the power spectrum of the pressure. While a perfect match of the experimental power spectra was not achieved over the entire frequency domain, the agreement is

good in the regime of 10 to 45 Hz (highlighted in Fig. 13). Noting that this frequency regime covers the dominant natural frequencies of the vertical tail (which are in the range of 10 to 18 Hz), it is expected that the FUN3D computations will provide reliable pressure data for the prediction of structural responses of the vertical tails.

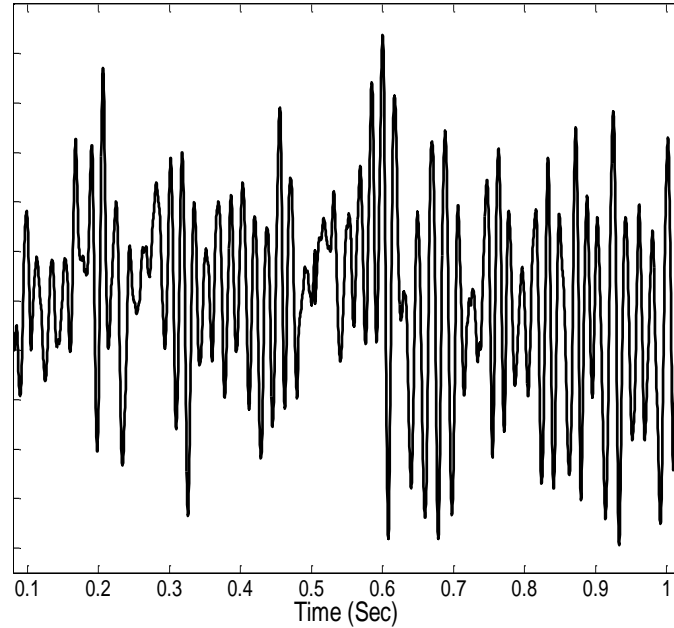


Figure 12. Sample time history of the pressure at point 1 [the location at 7% chord and 93% span. See Fig. 11(b)]. FUN3D computations with turbulence level=3.0.

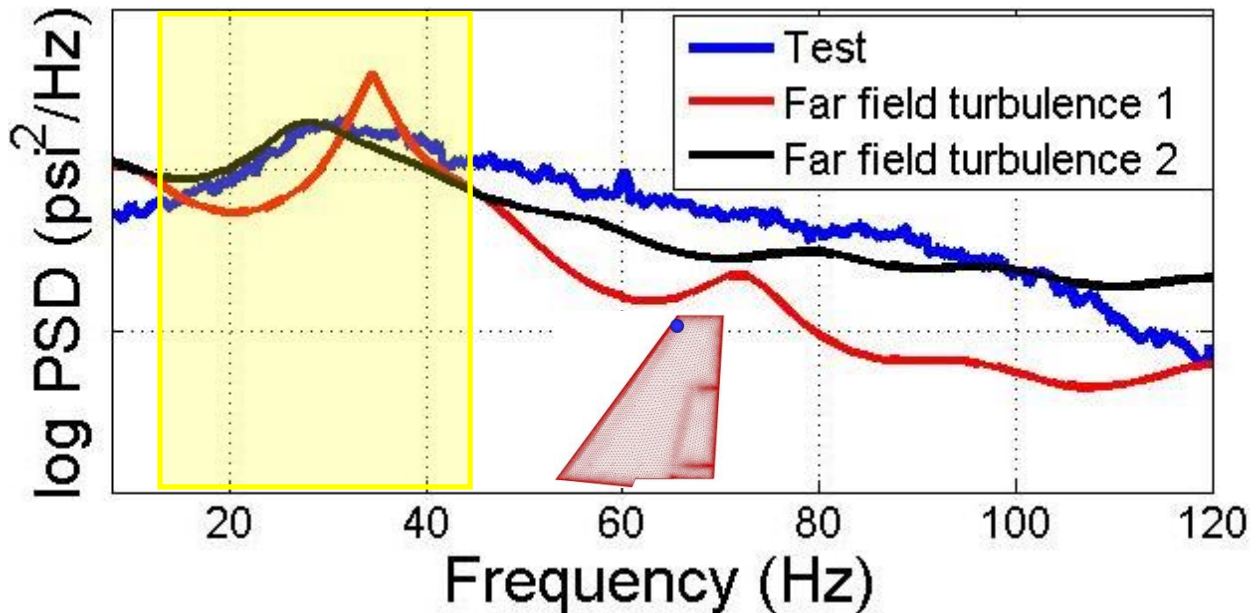


Figure 13. Power Spectral density of the pressure at point 1 [the location at 7% chord and 93% span. See Fig. 11(b)] from wind tunnel test and FUN3D computations with two different turbulence levels (Turbulence 1=1.34, Turbulence 2=3.0). Zone of interest for vertical tail vibration highlighted in yellow.

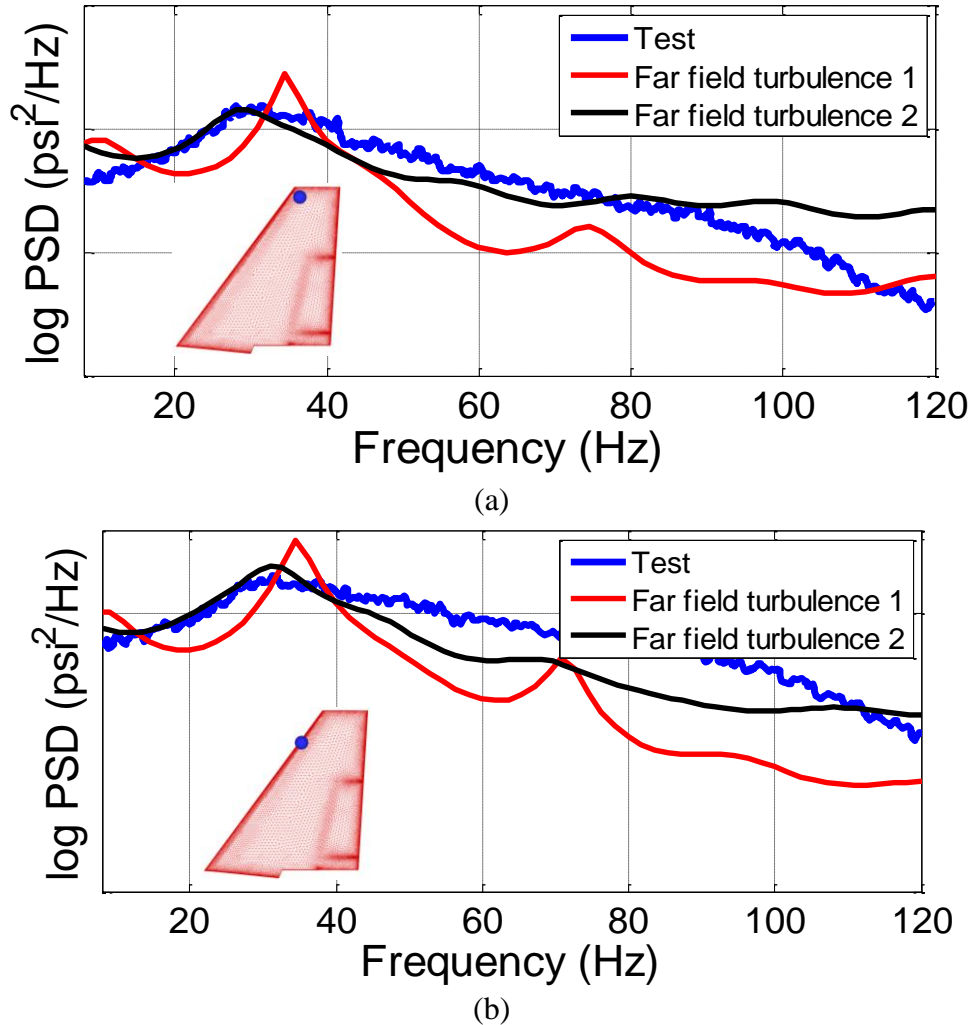


Figure 14. Power Spectral density of the pressure at (a) point 3 [the location at 23% chord and 93% span. See Fig. 11(b)], (b) point 7 [the location at 3% chord and 78% span. See Fig. 11(b)], from wind tunnel test and FUN3D computations with two different turbulence levels (Turbulence 1=1.34, Turbulence 2=3.0).

## 6. Conclusion

In this paper, the unstructured-grid flow solver, FUN3D, is used to compute the aerodynamic performance of F-15 and validated against available numerical and experimental results in the literature. In the computations, a half model of the F-15 aircraft with 14 million grid points is invoked for both steady and unsteady computations at high angles of attack. The Detached Eddy Simulation (DES) method based on the Spalart-Allmaras (SA) one-equation turbulence model is used.

For the transonic steady cases, the computational results of lift coefficients and pressure distributions for the vertical tail of F-15 at various angles of attack are compared with the wind tunnel measurement data, showing excellent agreement. Furthermore, to assess the capability of the detached eddy simulation method in FUN3D in predicting the fluctuating flow due to large flow separation, the benchmark problem of a cylinder in a cross flow is simulated. The time averaged pressure coefficient and skin friction coefficient distributions around the circumference

of the mid-plane of the cylinder, as well as the drag coefficient ( $C_D$ ), Strouhal number ( $St$ ), pressure in separation region ( $C_{pb}$ ), and separation angle on the cylinder ( $\theta_{sep}$ ) are compared with other numerical results and experimental measurements in the literature, and the agreement is very good.

Finally, the unsteady pressure fluctuations on the right vertical tail of F-15 at the angle of attack  $22^\circ$ , Mach number 0.09, and Reynolds number  $6.8 \times 10^5$  per feet (which format is needed for FUN3D), are computed using FUN3D, and their power spectral densities are compared with the wind tunnel measurements. The effect of the far field turbulence on the computational results is studied, and the optimal turbulence level is determined to capture the dominant regime of the power spectrum of the pressure. The FUN3D computation is thus expected to provide reliable pressure data for the prediction of the buffeting response of the vertical tail.

## References

- [1] Schmidt, S., and Oleg L., "Prediction of Aircraft Empennage Buffet Loads." *16th Australasian Fluid Mechanics Conference (AFMC)*, School of Engineering, The University of Queensland, 2007.
- [2] Morton, S.A., Russell M.C., and Kholodar, D.B., "High resolution turbulence treatment of F/A-18 tail buffet", *Journal of Aircraft*, Vol. 44, pp. 1769-1775, 2007.
- [3] Morton, S.A., et al. Detached-eddy simulations of full aircraft experiencing massively separated flows. AIR FORCE ACADEMY COLORADO SPRINGS CO DEPT OF AERONAUTICS, 2005.
- [4] McDaniel, David, et al. Comparisons of CFD solutions of static and maneuvering fighter aircraft with flight test data. AIR FORCE ACADEMY COLORADO SPRINGS CO, 2007.
- [5] Jeans, Tiger L., et al. "Lower-order aerodynamic loads modeling of a maneuvering generic fighter using DDES simulations." *7th AIAA aerospace sciences meeting*, AIAA-2009-0094, Orlando, FL. 2009.
- [6] Huttshell, L.J., Tinapple, J.A., and Weyer, R.M., "Investigation of buffet load alleviation on a scaled F-15 twin tail model", *Numerical Unsteady Aerodynamic and Aeroelastic Simulation* (1998).
- [7] Hanagud, S., F-15 Tail buffet alleviation: a smart structure approach. No. GIT-E-16-N32. Georgia Institute of Technology, Atlanta, Georgia, 1998.
- [8] Hanagud, S., Bayon de Noyer, M., Luo, H., Henderson D., and Nagaraja, K.S., "Tail Buffet Alleviation of High Performance Twin Tail Aircraft using Piezo-Stack Actuators", *40th AIAA/ASME/ASCE/AHS, Structures, Structural Dynamics and Materials Conference*, Vol. 2, pp. 1054-1064, 1999 (AIAA-99-1320)
- [9] Nagaraja, K.S., and Hanagud, S., "F-15 vertical Tail Buffet Alleviation: A smart Structures Approach", Rohini International and Airforce, Contract number WPAFB F 33615-96-C-3204, 1998.
- [10] Spalart, P.R. and Allmaras, S.R., "A One-Equation Turbulence Model for Aerodynamics Flows," AIAA Paper 92-0439, 1992.
- [11] Dacles-Mariani, J., Rogers, S., Kwak, D., Zilliac, G., and Chow, J., "A Computational Study of Wingtip Vortex Flowfield," AIAA Paper 93-3010, July 1993.
- [12] Vatsa, V., Lockard, D.P., and Khorrami, M.R., "Application of FUN3D Solver for Aeroacoustic Simulation of a Nose Landing Gear Configuration," AIAA Paper 2011-2820, June 2011.

- [13] Krishnan, V., Squires, K.D., and Forsythe, J.R., "Prediction of the Flow around a Circular Cylinder at High Reynolds Number," AIAA Paper 2006-901.
- [14] Roshko, A., "Experiments on the Flow past a Circular Cylinder at Very High Reynolds Number," *Journal of Fluid Mechanics*, Vol. 10, No. 3, pp. 345–356, 1961.
- [15] van Nunen, J., "Pressure and Forces on a Circular Cylinder in a Cross flow at High Reynolds Numbers," *Flow Induced Structural Vibrations*, Springer-Verlag, Berlin, 1974, pp. 748–754.
- [16] Travin, A., Shur, M., Strelets, M., and Spalart, P., "Detached-eddy simulations past a circular cylinder," *Flow, Turbulence, and Combustion*, Vol. 63, pp. 293–313, 1999.
- [17] Hansen, R., and Forsythe, J., "Large and Detached Eddy Simulations of a Circular Cylinder Using Unstructured Grids," AIAA Paper 2003-0775.
- [18] Triplett, W.E., "Pressure Measurements on Twin Vertical Tails in Buffeting Flow," *Journal of Aircraft*, Vol. 20, No. 11, pp. 920-925, 1983.
- [19] Ferman, M.A., and Turner, E.W., *An Experimental Investigation of Tangential Blowing to Reduce Buffet Response of the Vertical Tails of an F-15 Wind Tunnel Model. Volume 1. Test Results, Discussion and Correlation*, Report AFRL-VA-WP-TR-1999-3018, 1999.